

# A new method to estimate dark matter halo concentrations

Christian Poveda<sup>1</sup> & Jaime E. Forero-Romero<sup>1</sup>

<sup>1</sup>*Departamento de Física, Universidad de los Andes, Cra. 1 No. 18A-10, Edificio Ip, Bogotá, Colombia*

21 January 2015

## ABSTRACT

asd

**Key words:** methods: numerical, galaxies: haloes, cosmology: theory, dark matter

## 1 INTRODUCTION

In the concordance cosmology paradigm the the matter content of the Universe is dominated by dark matter which behaves as a collisionless fluid under the influence of gravity. In the last three decades numerical experiments have made possible the simulation of dark matter dominated universes, yielding valuable insights on the large scale structure formation process as depicted in observations.

One of the most striking results of these simulations is that dark matter clumps on galactic scales follow a universal density profile which in a first approximation is spherical symmetric and only dependent on the radial coordinate. These profiles seem to be universal; independent of the cosmological parameters and self-similar for different spatial scapes after an addequate re-scaling is applied.

One the most common parameterization of this density is known as the Navarro-Frenk-White (NFW) profile (Navarro et al. 1997). This profile is a double power law in radius, where the transition between the two happens at the so-called scale radius  $r_s$ . The ratio between the scale radius and the virial radius of the halo  $R_v$  is known as the concentration  $c = R_v/r_s$ , a quantity that has been found to be correlated with the halo mass.

The relationship between halo mass and concentration is in principle accesible to observations and provides a potential test of LCDM on galactic scales. With this promise a great deal of effort has been invested in calibrating this relationship with simulations but also finding the best possible way to constraint it with observations.

From the computational point of view there are two main methods to estimate the concetration parameter of a dark matter halo in a N-body simulation. The first method takes the particles composing the halos and bins them in logarithmic radii to estimate the density in each bin, then it proceeds with a fit of this density estimation as a function of radius. A second method uses an analytical property of the NFW that related the maximum of the ratio of the circular velocity to the virial velocity. In this method at each particle radius this ratio is estimated to find the maximum value for

this ratio; this value is used to find the roots of an equation which represent the concentration parameter.

The first method although is straightforward to apply has two main disadvantages. First of all it requires a large number of particles in order to have a proper density estimate in each bin. For a very low number of particles is hard to define a large number of bins to proceed with the fit. The second problem is that, as in any process involving data binning, there is not an way to estimate the optimal bin size, which in turn can affect the results of the fit.

The second method solves the two problems mentioned above. It works with low particles numbers and does not involve data binning. However, it effectively takes into account a single data point and discards the behaviour of the ratio  $V_{circ}/V_{vir}$  below and above its maxima.

In this paper we propose a new method to estimate the dark matter halo concentration from N-body simulation results. This method has two advantages with respect to the methods mentioned above. First, it does not involve data binning. Second, it does not throw away data points. Third, it allows for an straightforward estimation of the uncertainties in the concentration parameter.

Our method consists in building the cumulative mass profile from the particle data in the N-body simulation to find the best possible concentration value using a Markov Chain Monte Carlo methodology by comparing the data against the analytical expectation.

This paper is structured as follows. In Section 2 we review the basic properties of the NFW density profile and define the basic notation for the rest of the paper. Next in Section 3 we present our new method to estimate the halo concentration, payin special attention to the bayesian framework to find the most probable value and its uncertaintt. In Section ?? we demonstrate the power of our method with two different halo samples; the first one generated under controlled conditions and the second taken from a cosmological N-body simulation. Next in 5 we discuss these results by comparing them against other methods to estimate the concentration and comment on the consequences for the

concentration-mass relationship. We present our conclusions in Section 6.

## 2 BASIC PROPERTIES OF THE NFW DENSITY PROFILE

### 2.1 Density profile

The NFW density profile can be written as

$$\rho(r) = \frac{\rho_c \delta_c}{r/r_s (1 + r/r_s)^2}, \quad (1)$$

where  $\rho_c \equiv 3H^2/8\pi G$  is the Universe critical density,  $\delta_c$  is the halo dimensionless characteristic density and  $r_s$  is known as the scale radius, the radius that marks the transition between the power law scaling  $\rho \propto r^{-1}$  for  $r < r_s$  and  $\rho \propto r^{-3}$  for  $r > r_s$ .

We define the virial radius of a halo,  $r_v$ , as the boundary of the spherical volume that encloses a density of  $\Delta_h$  times the average density of the Universe. The corresponding mass  $M_v$ , the virial mass, can be written as  $M_v = \frac{4\pi}{3} \bar{\rho} \Delta_h r_v^3$ .

### 2.2 Integrated Mass

From these definitions we can compute the total mass enclosed inside a radius  $r$ :

$$M(< r) = 4\pi \rho_c \delta_c r_s^3 \left[ \ln \left( \frac{r_s + r}{r} \right) - \frac{r}{r_s + r} \right]. \quad (2)$$

We express the same quantity in terms of dimensionless variables  $x \equiv r/r_v$  and  $m \equiv M(< r)/M_v$ ,

$$m(< x) = \frac{1}{A} \left[ \ln(1 + xc) - \left( \frac{xc}{xc + 1} \right) \right], \quad (3)$$

where

$$A = \ln(1 + c) - \left( \frac{c}{c + 1} \right), \quad (4)$$

and the parameter  $c$  is known as the concentration  $c \equiv r_v/r_s$ .

From this normalization value and for later convenience we define the following function

$$f(x) = \ln(1 + x) - \left( \frac{x}{x + 1} \right). \quad (5)$$

The most interesting feature of Eq. (3) is that the concentration is the only free parameter to describe the density profile. In Figure 1 we show  $m(< x)$  as a function of  $x$  for different values of the concentration in the range  $1 \leq c \leq 20$ .

### 2.3 Circular velocity

It is also customary to express the mass of the halo in terms of the circular velocity  $V_c = \sqrt{GM(< r)/r}$ . From this we can define a new dimensionless circular velocity  $v(< x) \equiv V_c(< r)/V_c(< r_v)$ , using the result in Eq. 3 to have:

In Figure 2 we show the circular velocity profile for the same concentrations as in Figure 1.

$$v(< x) = \sqrt{\frac{1}{A} \left[ \frac{\ln(1 + xc)}{x} - \frac{c}{xc + 1} \right]}, \quad (6)$$

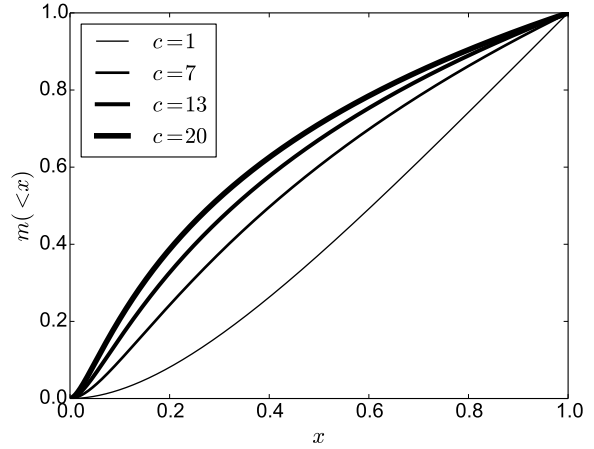


**Figure 1.** Dimensionless mass profiles as a function of the dimensionless radius for different concentration values.

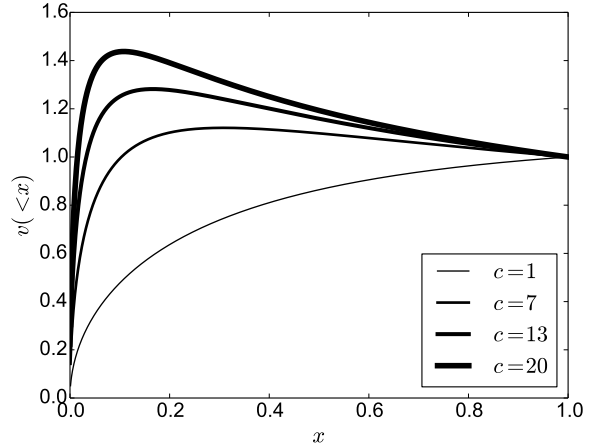


**Figure 2.** Dimensionless velocity profiles as a function of the dimensionless radius for different concentration values.

this normalized profile always shows a maximum provided that the concentration is larger than a values of  $c > ???$ . It is possible to show that for the NFW profile the maximum is provided by

$$\max(v(< x)) = \sqrt{\frac{c}{x_{\max}} \frac{f(x_{\max})}{f(c)}}, \quad (7)$$

where  $x_{\max} = 2.163$  and the function  $f(x)$  was defined in Eq. (5).

## 3 A NEW APPROACH TO ESTIMATE THE HALO CONCENTRATION

As we saw in the previous sections, once the density profile is expressed in dimensionless variables the only free parameter in the density profile is the concentration. There are two

main methods to estimate concentrations in dark matter halos extracted from N-body simulations.

The first method tries to directly estimate the density profile. It takes all the particles in the halo and bins them in the logarithm of the radial coordinate from the halo center. Then, it estimates the density in each logarithmic bin counting the particles and dividing by the corresponding shell volume. At this point it is possible to make a direct fit to the density as a function of the radial coordinate. This method has been most recently used by Ludlow et al. (2014) to study the mass-concentration-redshift relation of dark matter halos using the Millennium Simulation Series.

A second method uses the circular velocity profile. As it was shown in Fig. (2) the circular velocity shows a maximum for all profiles with concentration values larger than  $c > 2$ . The method finds the value of  $x$  for which the normalized circular velocity  $v(< x)$  shows a maximum. Using this value it solves numerically for the corresponding value of the concentration using Eq. (7). This method has been most recently used by Klypin et al. (2014) to study the mass-concentration-redshift relation using the Multidark Simulation Suite.

Our method is a third option that uses the integrated mass profile. First we define the center of the halo to be at the position of the particle with the lowest gravitational potential. Then we rank the particles by their increasing radial distance from the center. From this ranked list of  $i = 1, N$  particles, the total mass at a radius  $r_i$  is  $M_i = i \times m_p$ , where  $r_i$  is the position of the  $i$ -th particle and  $m_p$  is the mass of a single computational particle. In this process we discard the particle at the center.

We stop the construction of the integrated mass profile once we arrive at an average density of  $\Delta_h \bar{\rho}$ , with  $\Delta_h = 740$ , roughly corresponding to 200 times the critical density. This radius marks the virial radius and the virial mass. We divide the enclosed mass  $M_i$  and the radii  $r_i$  by these virial values to obtain the dimensionless variables  $m_i$  and  $x_i$ .

The construction of the numerical integrated mass profile has the advantage that it does not involve any binning and uses the information from all the particles in the halo, unlike the method that tries to directly build. Furthermore, as it will be clear in the next paragraph, the fit of this computational profile to the analytic expectation uses the information from all points, not only a single maxima point as the method using the circular velocity profile.

We use a Metropolis-Hastings algorithm to sample the likelihood function distribution defined by  $\mathcal{L}(c) = \exp(-\chi^2(c)/2)$  where the  $\chi^2(c)$  is written as

$$\chi^2(c) = \sum_{i=1}^N [\log m_i - \log m(< x_i; c)]^2, \quad (8)$$

where  $m(< x_i; c)$  corresponds to the values in Eq.(3) at  $x = x_i$  for a given value of the concentration parameter  $c$  and the  $i$  index sums over all the particles in the numerical profile.

For the walk in the Metropolis-Hastings algorithm we used 50000 steps where each step was randomly generated with a normal distribution centered around the last step with a standard deviation of  $\sigma = 0.03$ . From the  $\chi^2$  distribution we find the optimal value of the concentration and its associated uncertainty.

## 4 RESULTS

In this Section we present the results of applying our method on two different halo samples.

The first sample is composed by mock halos generated to have known concentration values in perfect spherical symmetry following an NFW profile. We use this sample to check that we can recover the expected values but also gauge the impact of the number of particles on the outcomes and the difference with respect to the two other fitting methods.

The second sample comes from a publicly available N-body cosmological simulation. From this sample we quantify again the differences between all the methods we have to fit the data. We also estimate the possible impact of the different methods in estimating the mass-concentration relationship from simulations.

### 4.1 Tests on Mock Halos

The method we use to generate the halos is based on the integrated mass profile. We start by fixing the desired concentration  $c$  and total number of particles  $N$  in the mock halo. With this values we define the mass element as  $\delta m = 1/M$ , corresponding to the mass of each particle such that the total mass is one. Then for each particle  $i = 1, \dots, N$ , we find the value of  $r_i$  such that the difference

$$m(< r_i; c) - i \cdot \delta m \quad (9)$$

is zero using Ridders' method.

The value of  $r_i$  is the radius of the  $i$ -th particle of the mock halo. Then we generate random polar and azimuthal angles  $\theta$  and  $\phi$  for each particle to ensure spherical symmetry. Finally these three spherical coordinates are transformed into cartesian coordinates  $(r, \theta, \phi) \rightarrow (x, y, z)$ .

We generate in total 400 mock halos splitted into four different groups of 100 halos each. The four groups differ in the total number of particles for their halos: 20, 200, 2000 and 20000. Inside each group the halos have random concentration values in the range  $1 < c < 20$  with a flat distribution. For all these halos we find the concentration values using the density, velocity and mass methods described in the previous section. We quantify the difference between the expected  $c_{in}$  and obtained  $c_{out}$  values by  $D = (c_{in} - c_{out})/c_{in}$ .

#### 4.1.1 The impact of particle number

Figure 3 shows the integrated distribution for  $D$  for the fits using our method, splitted into four different groups according to the particle number. From this Figure the first immediate conclusion is that increasing the number of particles increases the chances to recover the input values.

We believe that the main effect that contributes to this trend is that the particle that our algorithm finds to be the halo center (where the potential is minimum) gets closer to the original geometrical center (where no particle sits by construction) used to generate the halo. Poissonian noise makes this center fluctuate, changing the numerical radial profile from the analytical input.

For particle number of 20 the offset between the input and output concentration can be as large as 20%, with a slight bias around  $-0.05\%$ , i.e. the output concentration

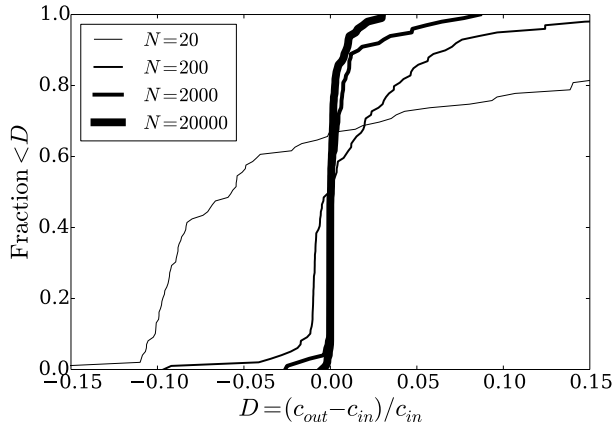


**Figure 3.** Cumulative distribution of the fractional difference,  $D$ , between the input concentration in the mock halo generator,  $c_{in}$  and the measurement by our MCMC code,  $c_{out}$ . Each curve corresponds to halos generated with a different number of particles,  $N$ .

is biased towards lower values than the input. For particle numbers of 2000 most of the offsets fall below 5%, with a clear peak around 0% indicating that any appreciable bias is absent.

#### 4.1.2 The impact of the input concentration

Hace falta hacer una figura para este caso.

## 4.2 Simulation Data

We use data from the MultiDark cosmological volume. This simulation follows the non-linear evolution of a dark matter density field sampled with  $2048^3$  particles over a cubic box of  $1000 h^{-1}\text{Mpc}$  on a side. The data is publicly available, more details about the structure of the database and the simulations can be found in (Riebe et al. 2013).

We select a sample of halos in a cubic sub-volume of  $100 h^{-1}\text{Mpc}$  on a side centered on the most massive halo in the simulation at  $z = 0^1$ . We select first all the halos at  $z = 0$  detected with a Friends-of-Friends (FoF) algorithm with masses in the interval  $10^{11} \leq M_{\text{FoF}}/h^{-1}\text{M}_{\odot} \leq 10^{15}$ . The FoF algorithm ran with a linking length of 0.17 times the average interparticle distance. This choice translates into an overdensity  $\Delta_h \sim 400 - 700$  that is dependent on the halo concentration (More et al. 2011).

For each selected halo with the previous procedure we select from the database all the particles that belong to it. From the particles we follow the procedure spelled out in Section 3 with  $\Delta_h = 740$  (corresponding to 200 times the critical density) to find the halo concentration. Finally, we store the values obtained for the virial radius, virial mass and concentration.

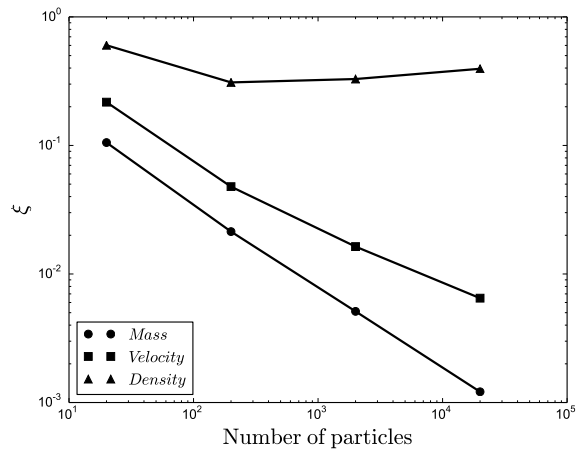


**Figure 4.** Relative error against number of particles

## 5 DISCUSSION

### 5.1 Comparison against other methods

We compared this method against two methods: The first one consists in using shells for estimating the density in function of the radius and using the same MCMC method for fitting and the second one consists in using the circular velocity  $V(r) = \sqrt{GM(<r)/r}$  and the relation for the NFW profile

$$\frac{V_{max}}{V(r_v)} = \sqrt{\frac{0.216c}{M(r_v; c)}} \quad (10)$$

Where  $V_{max}$  is the maximum velocity, to find the value of the concentration. We tested the three methods using the same data from the Mock Halos test. In order to see the accuracy of each method depending on the number of particles we define

$$\xi(n) = \frac{1}{|\mathcal{H}_n|} \sum_{\mathcal{H}_n} \left| \frac{c_{org} - c_{obt}}{c_{org}} \right| \quad (11)$$

Where  $\mathcal{H}_n$  corresponds to the set of haloes with  $n$  particles,  $c_{org}$  and  $c_{obt}$  are the original and obtained concentrations respectively for each halo in  $\mathcal{H}_n$  and  $|\mathcal{H}_n|$  the number of haloes in  $\mathcal{H}_n$ . Then we calculate  $\xi$  for each number of particles (20, 200, 2000 and 20000).

In Figure 4 we plotted  $\xi$  for the three methods. We consider that  $\xi$  is a good estimate because it is standardized, giving equal weight to all errors regardless of the magnitude of the concentrations or the number of halos. On the other hand we have that  $\xi$  decreases quite fast with the number of particles for our method and is more precise in any case than the other methods. As mentioned in FIXME “for a large fraction of halos, and for the most massive in particular, the NFW functional does not Represent a good fit to the density profile.” This fact could explain why  $\xi$  increases with the number of particles for the density method.

We also used these three methods to obtain the concentration for each halo in miniMDR1 and compared the results. As can be seen in Figure 5 the three methods show

<sup>1</sup> This corresponds to the miniMDR1 database in the MultiDark webpage

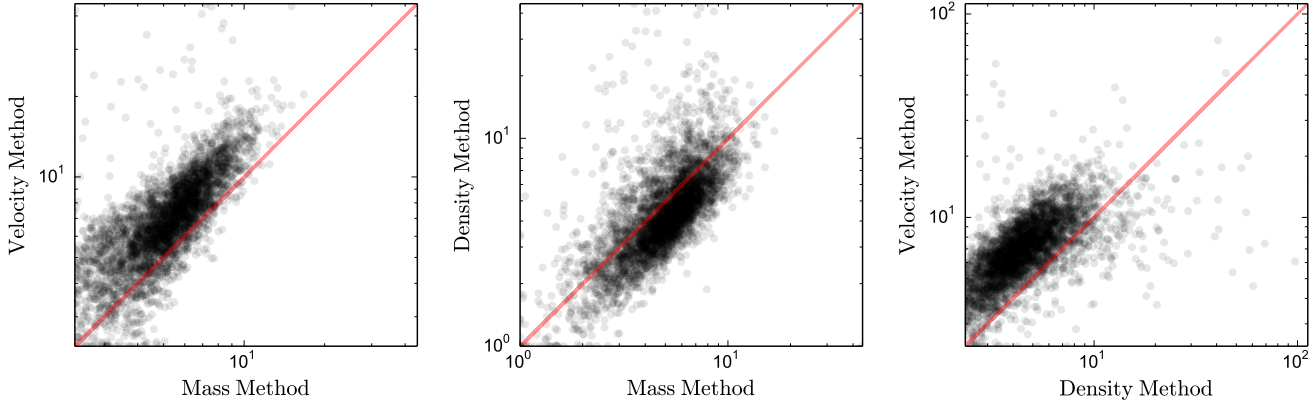


**Figure 5.** Comparison between the obtained concentrations by the three methods

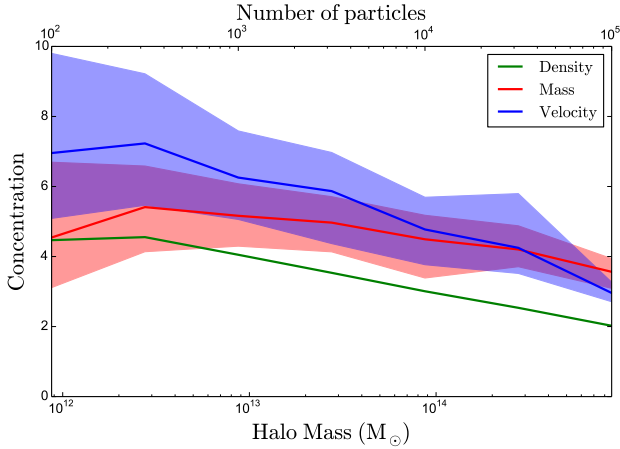


**Figure 6.** Concentration against number of particles

mutually consistent results. However it can be inferred that the concentration values obtained by the method of circular velocity are higher than those obtained by our method, and also the values obtained by the density method are generally below the results of our method.

Running another test with halos whose concentrations vary as a normal distribution of variance  $\sigma^2$  we found that the concentrations obtained by the method of circular velocity are a 35% greater than the ones obtained by the density method. However the concentrations obtained by the velocity method are barely higher (around 2% or 3%) than the ones obtained by our method. We did not find any significant variation in the concentration values obtained by any method by changing  $\sigma^2$  in contrast with FIXME.

## 5.2 Impact on the mass-concentration relationship

Additionally we compared those three methods plotting the concentration as a function of the number of particles of each halo

The bold lines in Figure 6 corresponds to the median and the thinner lines corresponds to the quartiles. Showing that our method has values ranging from those obtained

from the other two methods. Also we can see that the concentration obtained by the velocity method is higher than that obtained by the density method, this fact is consistent with FIXME.

## 5.3 Implication for comparisons against observations

FIXME: Ask Jaime

## 6 CONCLUSIONS

FIXME: Ask Jaime

## REFERENCES

- Klypin A., Yepes G., Gottlöber S., Prada F., Hess S., 2014, ArXiv e-prints
- Ludlow A. D., Navarro J. F., Angulo R. E., Boylan-Kolchin M., Springel V., Frenk C., White S. D. M., 2014, MNRAS, 441, 378
- More S., Kravtsov A. V., Dalal N., Gottlöber S., 2011, ApJS, 195, 4
- Navarro J. F., Frenk C. S., White S. D. M., 1997, ApJ, 490, 493
- Riebe K., Partl A. M., Enke H., Forero-Romero J., Gottlöber S., Klypin A., Lemson G., Prada F., Primack J. R., Steinmetz M., Turchaninov V., 2013, Astronomische Nachrichten, 334, 691
- <http://adsabs.harvard.edu/abs/2014ApJ...795..163U>
- <http://adsabs.harvard.edu/abs/2012ApJS...199...25P>
- Figura 3!